Molecular design rules for imparting multiple damping modes in dynamic covalent polymer networks

Laura E. Porath[1,2], Nabil Ramlawi[3], Junrou Huang[2,4], M.T. Hossain[3], Maryanne Derkaloustian[1], Randy H. Ewoldt[2,3,5], Christopher M. Evans[1,2,5]*

[1] Department of Materials Science and Engineering, University of Illinois Urbana Champaign
[2] Frederick Seitz Materials Research Laboratory, University of Illinois Urbana Champaign
[3] Department of Mechanical Science and Engineering, University of Illinois Urbana Champaign
[4] Department of Chemistry, University of Illinois Urbana Champaign
[5] Beckman Institute, University of Illinois Urbana Champaign

*Corresponding Author: evans365@illinois.edu

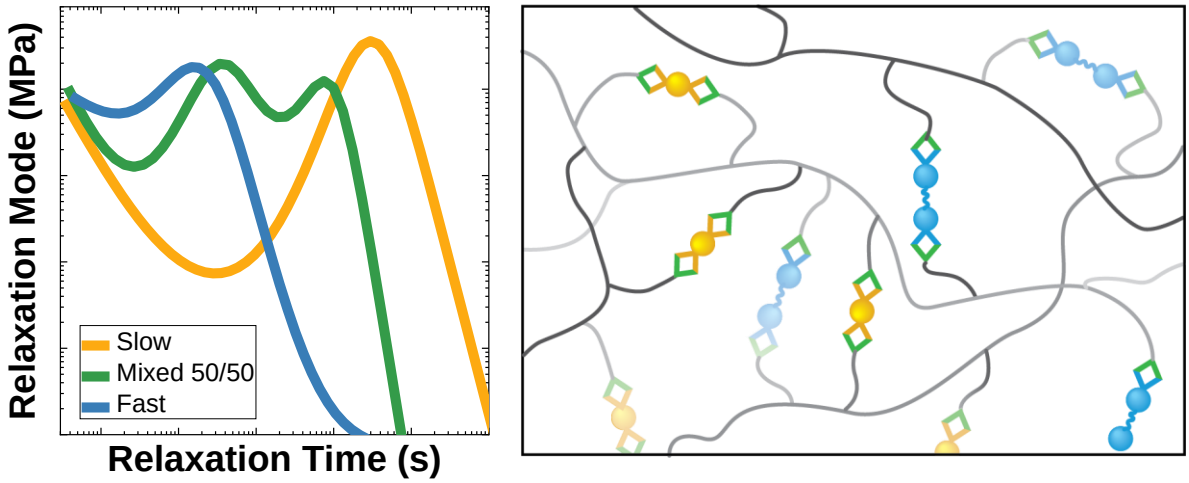

Introduction

The complex viscoelastic response of polymers is critical to their function and performance in applications[1] spanning additive manufacturing[2, 3], self-healing polymers[4, 5], actuators[6, 7], electrolytes[8, 9], adhesives[10], and damping materials.[11] A common way to quantify this response is using oscillatory mechanical spectroscopy or rheology, where the sample is deformed over a range of controlled frequencies, and the storage (G') and loss (G'') moduli are measured and reflect the relative solid-like and liquid-like response, respectively. The change in the ratio of G''/G', or tan δ, then reveals how the sample transitions from solid- to liquid-like behavior as a function of

temperature or experimental timescale. The frequency of these peaks also determines the ability of a polymer to damp sound and vibration waves.[12] Achieving specific shapes of tan δ spectra, including the number, shape, and breadth of peaks, is a grand challenge in soft matter design. Dynamic polymer networks have emerged as a promising route to imparting multiple relaxation modes into polymers by introducing timescales of bond exchange in addition to the existing polymer dynamics.[13] Dynamic bonds are an essentially orthogonal route to traditional polymer design, distinct from controlling the glass transition, melting temperature, copolymer composition, polymer architecture, or phase separation (both micro and macroscale). For damping materials such as in acoustic chambers or washing machines, the frequency of the relaxation spectrum peak indicates which vibration and sound waves can be dampened. Current damping materials such as Sorbothane or hydrogels use a high quantity of plasticizers or solvent, which limits their broad applicability.

The understanding of how to rationally impart multiple, hierarchical dynamic modes into soft materials is still lacking. In hydrogels formed from 4-arm star backbones with metal-ligand interactions as crosslinkers, it has been reported that mixing two kinetically distinct dynamic bonds can lead to two distinct relaxation modes which vary in intensity (both not frequency) depending on the ratio of the two metal ion types which exhibit different binding kinetics.[13] Another study of 4-arm star hydrogels with dynamic covalent boronic ester crosslinks only lead to one intermediate mode in systems with two kinetically distinct crosslinks.[14] These two hydrogel results illustrate the knowledge gap in imparting multiple relaxation modes. In dry pendant crosslinked dynamic networks, a single mode was also observed in most mixed crosslinker cases.[15] The key question is what leads to such differences in nominally similar systems, and if they can be understood at the molecular level to enable the intentional design of hierarchical dynamics. Associative versus

dissociative exchange mechanisms for the dynamic crosslinks, the ability of the fast and slow bonds to rearrange in the metal-ligand system but not the boronic ester networks, the timescale separation of the bonds being combined into the networks, the number of dynamic bonds per backbone, or another yet unidentified factor are all potential culprits for the observed behavior. Polymer networks which independently test these hypothesized reasons for multiple hierarchical modes are needed to shed light on this aspect of dynamic design in soft materials.

Here, we synthesize dry acrylic polymer networks with multiple pendant diols capable of forming dynamic covalent boronic ester crosslinks. When bonded with either a fast or slow crosslinker, these vitrimers have a three orders of magnitude difference in their characteristic relaxation times determined from shear rheology frequency sweeps. A mixture of the two crosslinkers gives rise to two distinct modes. This result is in stark contrast to our prior work incorporating the same two crosslinkers into telechelic silicone networks,[16] which only show one intermediate relaxation peak. Comparing our results to previous work[13-15] on other dynamic network architectures, we hypothesize that the presence of multiple dynamic bonds along a backbone and the ability of dynamic bonds to randomize at each crosslink site are critical for creating multiple relaxation modes in a single polymer network.

Results

Hierarchical dynamics were designed into functionalized butyl acrylate polymers by crosslinking with two types of tetrafunctional boronic esters, which have orders of magnitude different kinetics and are referred to as “fast” and “slow” (**Figure 1a**). The fast crosslinker was chosen based on the work of Guan and coworkers,[18] and the slow crosslinker is commercially available. The system was determined to be fully crosslinked based on verification of molecular weight from GPC, the disappearance of free hydroxyl groups in the ATR-FTIR spectra, and from a sufficiently high rubbery plateau modulus (**Figure S1-S3**). Thermal characterization showed a glass transition temperature of -30 °C, and X-ray characterization showed some weak aggregation which was similar in the both the pure and mixed dynamic bond networks (**Figures S4-S6**). Time-lapse photos confirm that samples are viscoelastic liquids at room temperature (**Figures S7**) and bounce tests confirm elasticity with measurable dissipation at short time scales (**Figure S8**). To determine the detailed relaxation behavior of the fast, slow, and mixed networks, oscillatory shear rheology was conducted. The resulting frequency sweeps (**Figure 1b**) reveal a plateau modulus at high frequency and terminal flow regime at long times. A finite viscosity $\eta_0 = G''\omega$ exists for all samples at sufficiently low frequencies; corroborating evidence for η_0 comes from quantitative analysis of the gravity-induced time-lapse flow of initially spherical samples which extends the range of observed timescales to $t \sim 8{,}400$ s (**Figure S7, Figure S9,** and supporting analysis in SI). At higher frequencies, an elastically-dominated behavior is present, but with non-negligible loss modulus, G''. The non-negligible G'' is evident from bounce tests of samples that show minimal rebound with impact times ~10 ms corresponding to oscillatory frequency $\omega \sim 300$ rad/s (**Figure S8, Figure S9,** and supporting quantitative analysis in SI).

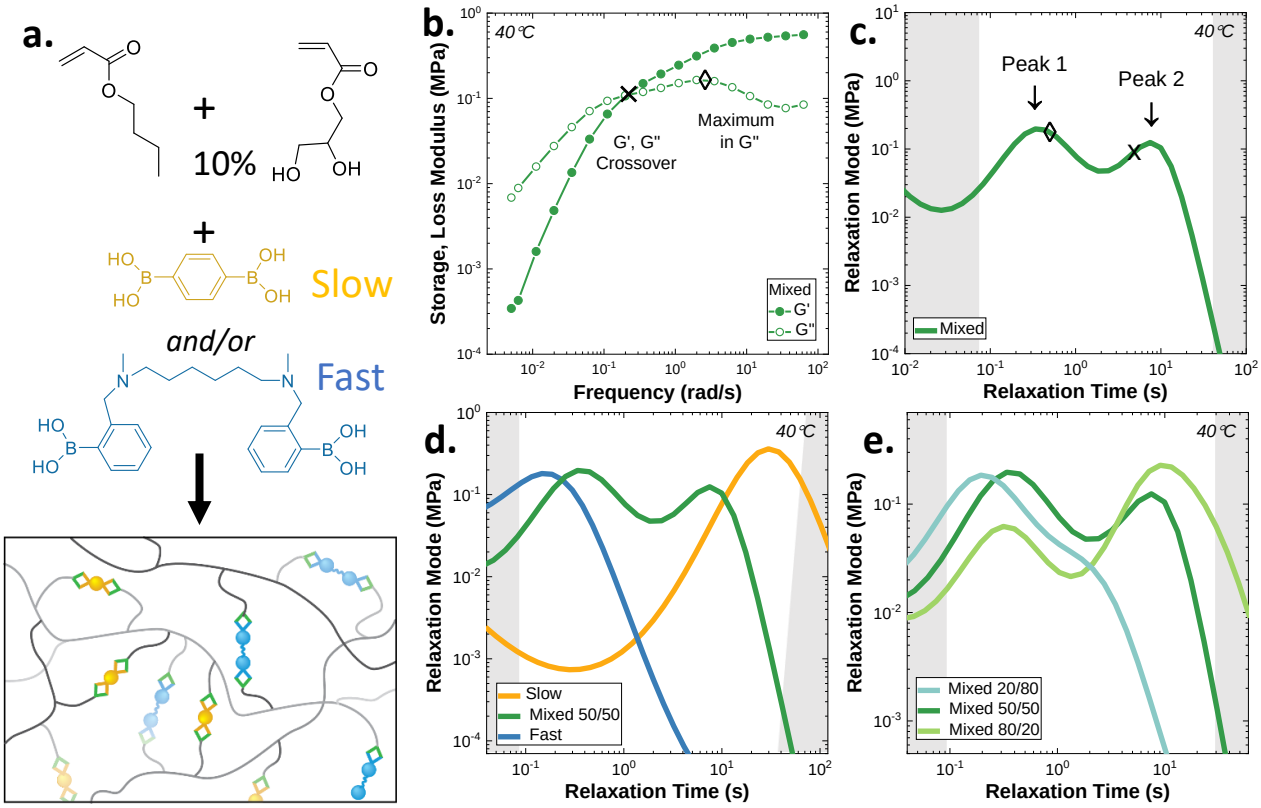

***Figure 1**: (a) Scheme of butyl acrylate polymerized with 10% diol-functionalized acrylate groups crosslinked with either a slow or fast boronic ester crosslinker (or both in the mixed system) to make a statistical dynamic polymer network. (b) Oscillatory shear rheology of the mixed acrylate network at 40°C showing two relevant timescale: the G', G" crossover, and the maximum in G". (c) The relaxation spectrum of the mixed network converted from the frequency data shows two peaks, representative of the fast and slow crosslinkers in the mixed network. The x and diamond refer to the peaks marked in (b). (d) The relaxation spectra of the slow, mixed 50/50, and fast crosslinked acrylate networks at 40°C show one peak for the single component systems and two peaks for the mixed. (e) Other mixed percentages of fast and slow crosslinkers also show two peaks with peak strength corresponding to crosslinker percentage. Regions in gray are outside of the limit of trustworthy data.*[17]

Detailed analysis of the frequency sweeps can identify characteristic timescales, such as the crossover timescale between the storage (*G'*) and the loss modulus (*G"*), present in all networks. In the frequency sweep of the mixed network (**Figure 1b**), an additional timescale can be identified at the maximum in the loss modulus at higher frequency. To quantitatively compare the distribution of relaxation modes, a relaxation spectrum is then inferred from the frequency sweeps for all networks as a high-density discrete spectrum (**Figure S10-12, Table S3-5**), found from nonlinear regularization fitting. The conversion from frequency sweep to relaxation spectrum limits the range of credible data, which is indicated by the gray regions in **Figures 1c-e**.[17] The two

peaks in the inferred spectrum of the mixed system (**Figure 1c**) correspond closely to the two timescales, denoted by a crossmark and a diamond, identified from the frequency sweep.

Further analysis of the spectra shows that these timescales correspond to the fast crosslinker (Peak 1, which corresponds to the maximum in G'' at higher frequency) and the timescale for flow (Peak 2, which is intermediate to the crossover times for the pure slow and fast networks). The relaxation spectra for the fast and slow single component networks, as well as the mixed fast and slow (50/50 molar percentage) network are shown in **Figures 1d and S13**. The pure component networks have three orders of magnitude difference in their peak relaxation time, as expected based on the large difference in bond exchange rates of the crosslinkers. The two peaks of the mixed network are in proximity to the peaks exhibited by the pure networks, indicating that the two peaks arise from contributions of the two crosslinkers. Additional evidence is provided in **Figure 1e and S14**, where changing the molar percentage of crosslinkers did not change the location of the peaks in the spectrum but did affect the peak strength. The mixed networks of 80/20, 50/50, and 20/80 (slow/fast) all show two peaks, and the peak height varies with the percentage of fast or slow crosslinker, highlighting the tunability of this system. This multi-modal result is not trivial and could not have been predicted a priori based on the chemistry. Previous work mixing the same crosslinkers in telechelic PDMS vitrimers reported only one combined relaxation peak.[16] Understanding how the architecture or polymer chemistry leads to these qualitatively distinct results is needed to intentionally impart hierarchical dynamics.

The relaxation behavior of the acrylate vitrimers was investigated over a frequency range of five decades and at temperatures from 20 – 80 °C (**Figure 2**). Both slow and fast networks show a Maxwellian terminal regime where $G' \sim \omega^2$ and $G'' \sim \omega$ in the limit of low frequency, a glassy upturn in the loss modulus in the limit of high frequency, and a rubbery modulus of similar

magnitude. Moreover, the local maximum of the loss modulus in the fast and slow networks coincides with the crossover of the storage (*G'*) and loss moduli (*G"*), unlike the mixed system. These observations show that these networks have a single dominant relaxation mode across all temperatures corroborating the single peak spectra shown in **Figure 1**. The peak of this dominant mode shifts toward faster times as temperature increases.

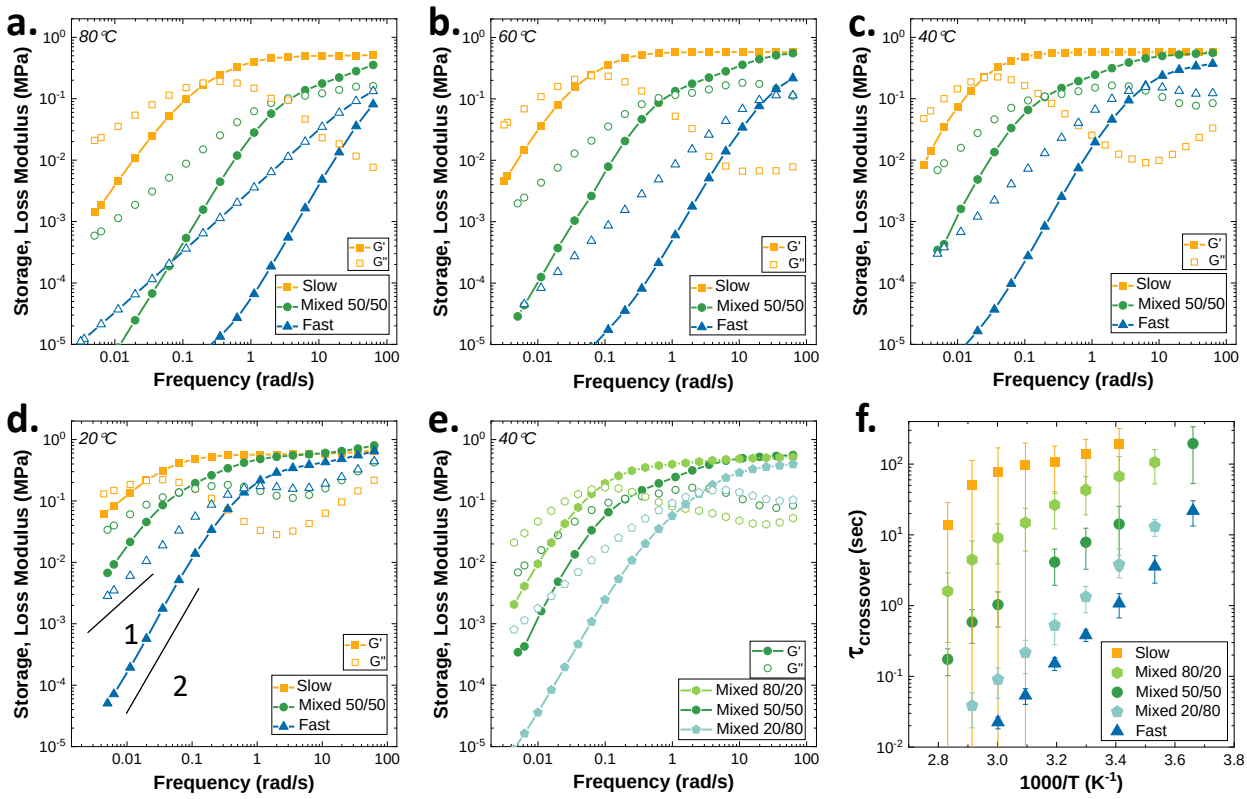

***Figure 2**: The oscillatory shear rheology data is shown at multiple temperatures for the slow, mixed 50/50, and fast acrylate crosslinked networks. (a) At 80°C, the fast crosslinker does not reach a crossover. (b) At 60°C, the mixed system shows non-Maxwellian behavior, and the fast system reaches a crossover. (c) The systems all shift to slower dynamics at 40°C as the materials get colder. (d) The terminal regimes of G'~ ω^2 and G"~ ω^1 are shown and agree with the fast crosslinker behavior. (e) The mixed systems of 80/20, 50/50, and 20/80 show correspondingly faster crossovers. (f) The relaxation time taken from the crossover of G' and G" are shown versus temperature for each acrylate vitrimer.*

The mixed crosslinker system (50/50 mole percentage) deviates from the typical Maxwell behavior of the pure component networks. Instead of a smooth transition from low to high frequency of a convex upturn of the storage modulus after the crossover, the storage modulus exhibits power law behavior at intermediate frequencies most clearly seen in **Figures 2b** and **2c**

from 1 – 10 rads/s. The intermediate regime between the crossover point and the rubbery plateau extends over 1 to 2 orders of magnitude of frequency in the mixed system, while spanning a half order of magnitude at most in the single crosslinker systems as shown in **Figures 2a–d**. The separation of timescales is imperative for evidence of contributions from both crosslinkers. This intermediate, power law regime is extended due to the orders of magnitude difference in crosslinker kinetics. The phenomenon of power law dependence has been previously identified as critical gel behavior in systems approaching their gelation point.[19] In these mixed acrylate boronic ester networks, the power law behavior does not arise from gelation kinetics but as a result of a regime where both crosslinker dynamics are important. In addition, the terminal regime follows Maxwellian terminal behavior which indicates the network is fully formed and not experiencing gelation kinetics.

As the temperature decreases, more of the plateau regime of the mixed and fast networks is accessible in the experimental range because the dynamic bonds slow down with decreasing temperature. The rubbery plateau converges for all three systems due to the nearly identical crosslink density of all three systems, and this is clearly visible at 20°C (**Figure 2d**). When the frequency or temperature at which the materials are probed is held constant, the materials can produce drastically different results, and the crosslinking can control whether the material behaves as a liquid, viscoelastic solid, or rubbery network (**Figure S3**). For the mixed networks with different crosslinker ratios (**Figure 2e**), the crossover is correspondingly faster (20/80) or slower (80/20) than the 50/50 slow/fast network. Moreover, these networks show a smaller intermediate region compared to the equal-ratio mixed system as their behavior is closer to the single component system.

To understand what sets the terminal relaxation timescales between networks, the crossover times are plotted against inverse temperature (**Figure 2f**). The fast and mixed networks exhibit Arrhenius behavior which is common for vitrimers and is expected when flow is controlled by a process with an Arrhenius temperature dependence, such as bond exchange. The activation energies for each network are calculated from the slopes in **Figure 2f** and range from 36 to 65 to 83 kJ/mol in the slow, mixed 50/50, and fast networks respectively (**Figure S15**) and the 80/20 and 20/80 mixed networks fall in between their respective pure components. The fast crosslinker appears to decrease the crossover time and increase the activation energy in the mixed networks, which indicates that the crossover frequency is not set entirely by the slow crosslinker and is a result of multiple relaxation kinetics. The timescale of relaxation may also affect bulk scale events such as bouncing, where the mixed system exhibits a higher bounce than the fast or slow networks suggesting comparatively lower tan δ at frequencies higher than what is available from shear rheometry in Figure 2 (**Figures S8-S9**).

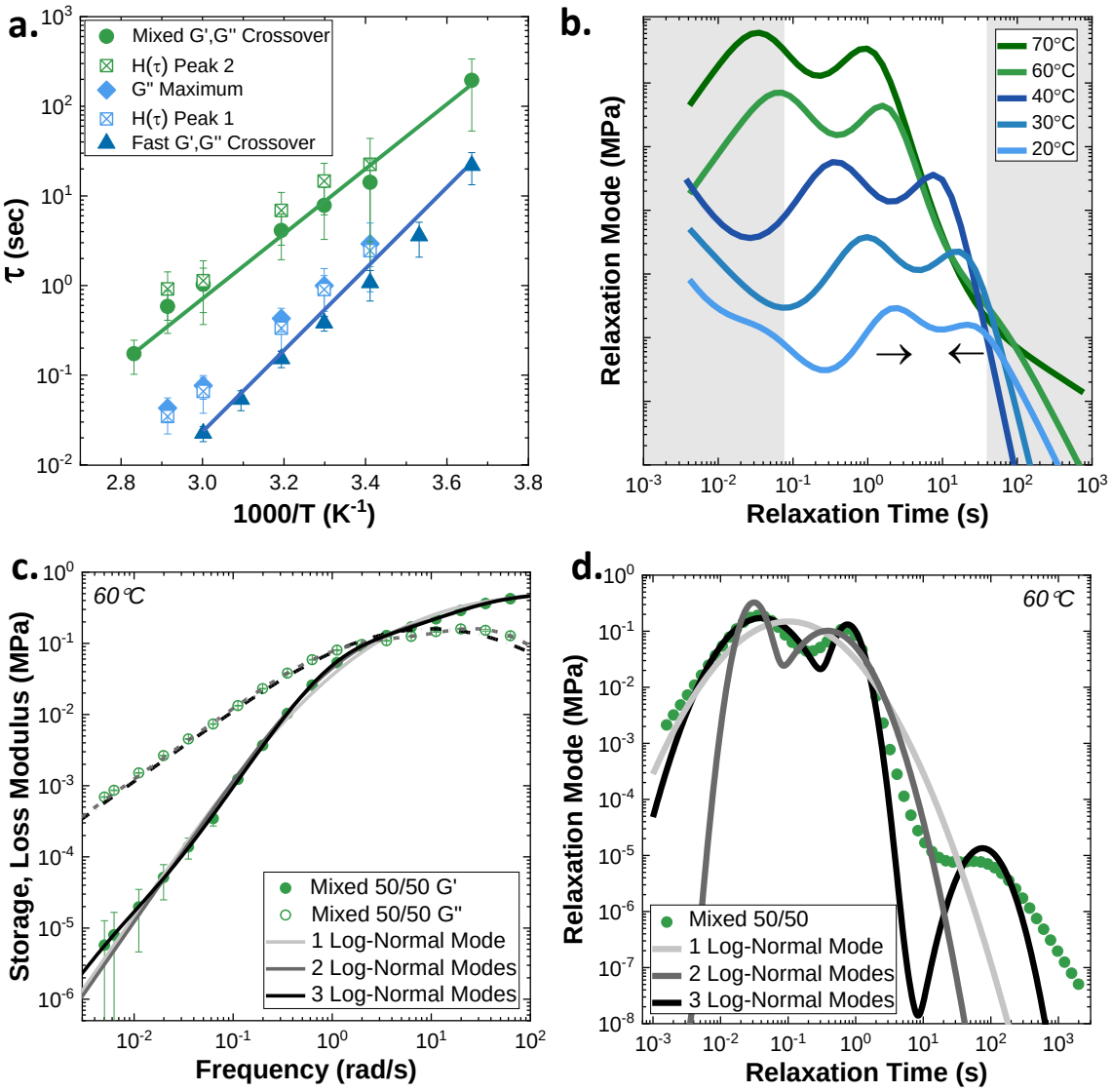

***Figure 3**: (a) Timescales for relaxation are compared using different metrics from frequency and relaxation spectra data and agree well. (b) The mixed 50/50 relaxation spectra are shown at multiple temperatures (shifted y axis for clarity) to show peak merging. (c) The dynamic moduli frequency sweep data for a mixed network at 60°C is fit by different models (solid lines are G' and dashed lines are G"). (d) Comparison of the spectra inferred from the 3 models shown in (c) to the TRIOS converted spectrum (green dots).*

In the mixed 50/50 vitrimer where two peaks in the relaxation spectrum are visible, the maxima of Peak 1 and Peak 2 are identified and then compared to the crossover timescales of the mixed and fast networks, as well as to the maximum of the loss modulus in the mixed network in **Figure 3a**. The slower peak in the relaxation spectrum (Peak 2) falls within error of the crossover relaxation time of the mixed network (**Figure 1c**). The *G"* maximum values of the mixed network

and the faster relaxation spectrum peak (Peak 1) agree well with the crossover times of the fast crosslinker network. This agreement indicates that Peak 1 arises from the relaxation of the fast crosslinker in the mixed networks, while Peak 2 is attributed to terminal relaxation of the network. Both crosslinkers must relax for the material to exhibit terminal behavior, and the lower concentration of slow crosslinkers leads to a faster terminal relaxation time.

Because the two peaks in the mixed vitrimer have distinct temperature dependencies, the behavior converges upon cooling, which points to temperature as a dial to control the separation of timescales in vitrimers (**Figure 3a**). The mixed network relaxation spectra at each temperature from 70 °C to 20 °C are shown in **Figure 3b** to clearly illustrate the merging of the two relaxation modes with decreasing temperature. In the present vitrimers, the T_g intervenes before the two peaks fully merge. Temperature therefore provides an additional handle for control of multimodal behavior.

Relaxation spectrum inference does not generate a unique solution, but a Bayesian inference perspective can quantitatively assess the credibility of different model fits.[20] The Bayesian Information Criterion (BIC) has been used as an estimate of full Bayes likelihood with rheological data fitting,[21-23] and here we use it to assess the credibility of the multi-peak spectra inferred from the TRIOS software. The TRIOS software produces a high-density discrete spectrum, found from nonlinear regularization fitting. The BIC is a metric used to choose the most credible model to fit a set of data, where the goodness of fit is balanced by a penalty to high number of parameters. BIC is calculated as

$$BIC = n_D \log\left(\frac{RSS_w}{n_D}\right) + n_p \log n_D,$$

where n_p is the number of parameters, n_D is the number of data points, and RSS_w is the best fit's residual sum of squares between the model prediction and the experimental data represented as *G'* and *G"* and weighted by the reference experimental value ($RSS_w = \sum_i^{n_D} \left(\frac{y_{i,M} - y_{i,D}}{y_{i,D}}\right)^2$).[24] Models with a lower BIC are regarded as more credible with an approximate relative probability $\sim e^{-\Delta BIC}$. We fit the dynamic moduli of the mixed system (50/50) at 60°C and compare the BIC of 3 parametrized continuous spectra models, which are the 1-mode, 2-mode and 3-mode log-normal distributions. Each log-normal mode $H_i(\tau)$ exhibits a normal distribution of $H_i(\tau) = H_{i,\max} e^{\frac{\left(\log\tau - \log\tau_{i,\max}\right)^2}{\sigma_i^2}}$ with a peak value $H_{i,\max}$ at a location time $\tau_{i,\max}$with a spread σ_i. Details about calculating moduli from spectra and the fitting algorithm used are discussed in the Supporting Information (**Figure S11**). The 3-mode log-normal was found to be the most credible with a BIC of -194, followed by 2-mode log-normal with -123 and 1-mode with -115. Moreover, the best fits of the 3 models shown in **Figure 3c** show that at least two modes are needed to capture the complex relaxation of the mixed system, especially in the intermediate regime. The existence of a third mode at $\tau > 10$s (**Figure 3d**) for the 3-mode log-normal distribution is needed to capture storage modulus data in the lower frequency regime. However, the high uncertainty of data in that region suggests that this peak is caused by instrumentation issues rather than a material response (check SI for details). The shape of the most credible spectrum agrees with the high-density discrete spectrum as shown in **Figure 3d,** supporting the use of the inferred spectra for this work. Results for the slow and fast crosslinker systems show that a single log-normal mode fits the data most credibly compared to two log-normal modes and the single mode Maxwell model (**Figure S11**). This result implies that a multi-peak distribution of relaxation times is necessary to capture

the response of these vitrimers consistent with the inferred, high-density discrete spectra in this work.

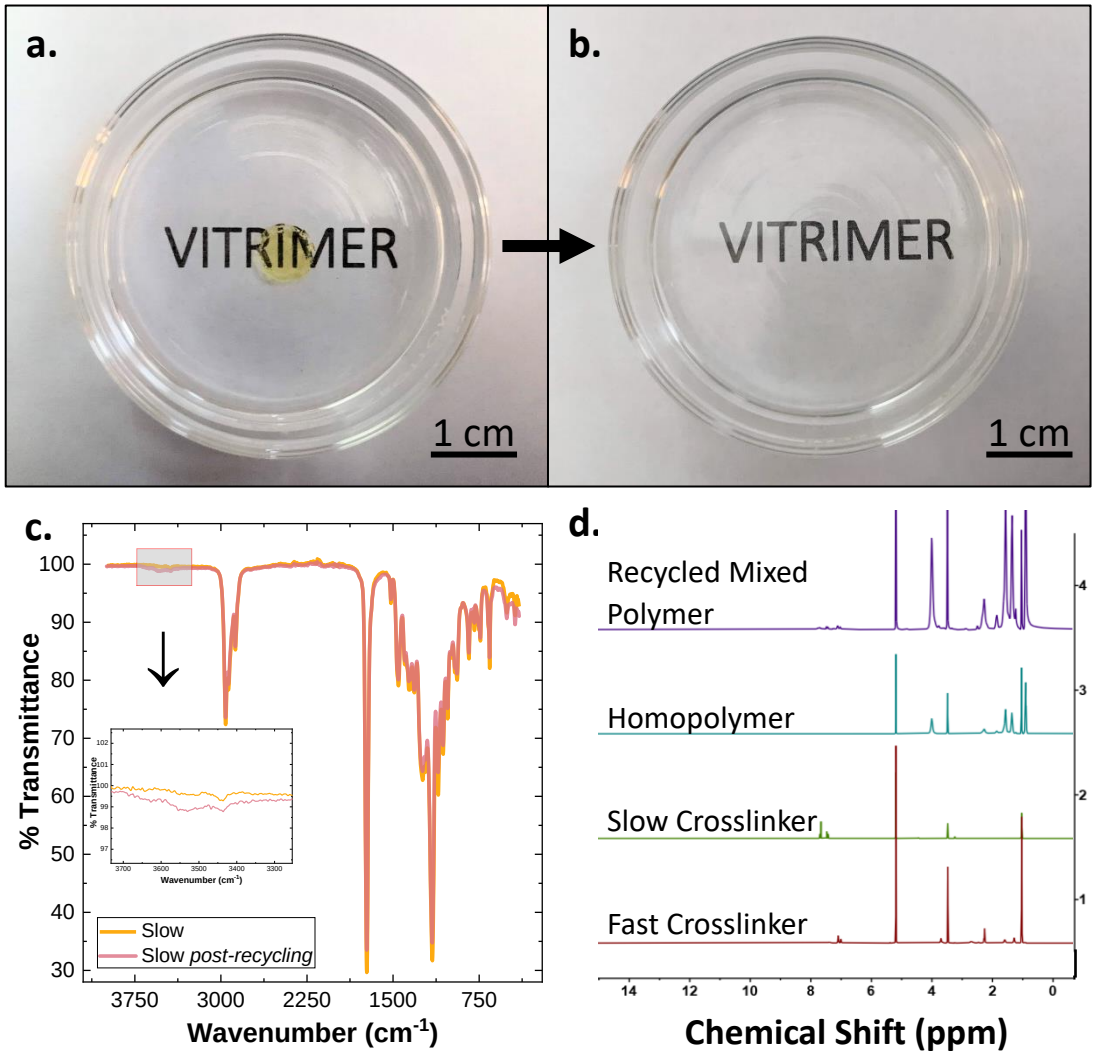

***Figure 4**: A slow crosslinked acrylate network is dissolved in a glass petri dish filled with 20mL ethanol. (b) The sample has fully dissolved after heating at 90°C for one hour. (c) FTIR of the slow network is shown before and after the recycling process. (d) A mixed network dissolved in d-ethanol shows similarities in ^{1}H NMR to its main components, the homopolymer and the fast and slow crosslinkers.*

A benefit of dynamically bonded networks is their ability to be reused, allowing for sustainability to be introduced to many applications where polymers would simply be discarded. Reprocessability, or the breaking up and reshaping, of vitrimers has been demonstrated in many systems.[25, 26] Recycling of dynamic materials is not always possible due to degradation of the

starting materials after dissolving in the solvent. The present acrylic boronic ester networks are both reprocessable and recyclable (**Figure 4a, b**). Ethanol dissolves 0.2 grams of this network in under 10 minutes and a less polar solvent, isopropyl alcohol, can dissolve the vitrimer in a few hours (**Figure S15**). Alcohols are able participate in bond exchange with the boronic esters to reduce the crosslink density and break down the network. The slow network was recovered after boiling off the solvent from the dissolved sample, and Fourier transformed infrared spectra was used to compare the starting and recycled materials (**Figure 4c**). The post-recycled network had slightly more free -OH groups (peak at 3400cm^{-1})[27] perhaps due to uncrosslinked chains or the loss of small molecules which alters the stoichiometry of network formation. Successful recycling was also confirmed with NMR when a mixed acrylate network was dissolved in deuterated ethanol (**Figure 4d**). The recycled polymer shows the major peaks of the homopolymer sample between 1-2ppm and, also, shows evidence of the presence of both fast and slow crosslinkers at 7 and 7.5ppm, which indicates little loss of the polymer backbone or crosslinkers occurred during recycling.

Discussion

Based on the existing literature and the present results, multiple aspects of polymer chemistry are important in the design of relaxation spectra with one or more dominant peaks. Literature examples that have pursued hierarchical dynamics are shown schematically in **Figure 5**. The metallogel with a 4-arm star crosslinked by metal-ligand interactions is shown with circle crosslinkers indicating the metal ions (**Figure 5a**).[13] This system showed multiple peaks with tunable intensity based on the percentage of two metal ions. A similar 4-arm star polymer network, with two boronic ester crosslinkers is represented in **Figure 5b**.[14] This material did not show multiple peaks in the relaxation spectra when crosslinkers were mixed but instead observed a

single peak which shifted position based on crosslinker percentage. Both were networks swollen with water.

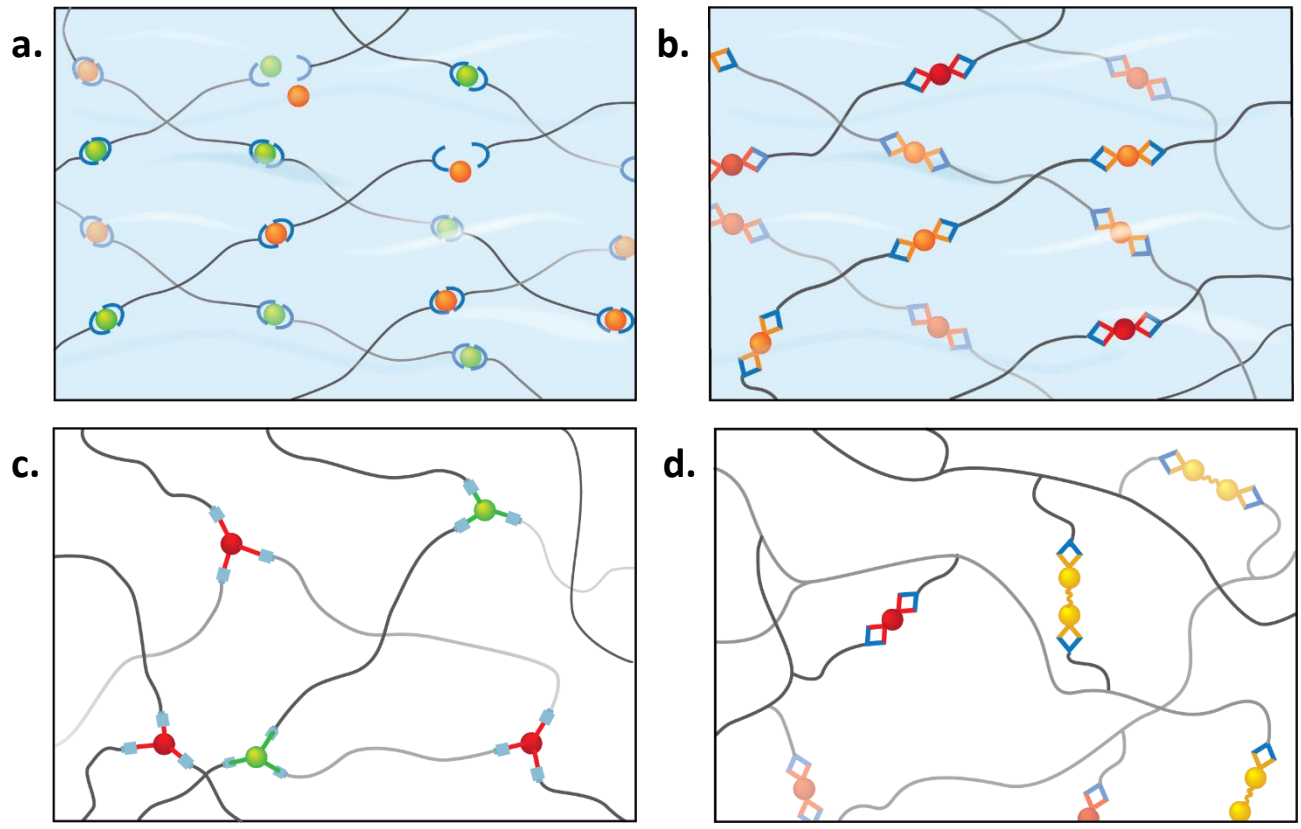

Figure 5*: Idealized cartoons of mixed crosslinker systems. Larger differences in color of the crosslinkers indicate corresponding differences in exchange kinetics. (a) Ionic bonds of different strengths in a hydrogel are able to bond to any free site. (b) Covalent tetrafunctional crosslinkers in a hydrogel have one crosslinker type per chain. (c) A telechelic vitrimer has dynamic covalent bonds of orders of magnitude different kinetics. (d) A statistical vitrimer has dynamic covalent bonds of low density and similar kinetics.*

Three potential reasons were considered to explain why mixing dynamic bonds does not always lead to two distinct peaks in the relaxation spectrum. The first is the difference in kinetics between the mixed crosslinkers which was approximately one order of magnitude smaller in the boronic ester hydrogel. This could have a significant impact on the timescale separation and therefore on multimodal behavior. Second, although both networks have the 4-arm star geometry, the metallogel has ions that can exchange with any bond site, while the boronic ester network has four arm stars with only fast or only slow crosslinkers. Therefore, each polymer strand will only

experience the exchange events of one type of crosslinker. Third, the metallogel relies on a dissociative chemistry while the boronic esters have an associative exchange mechanism. However, the present acrylate vitrimers (associative exchange) do show multiple modes, which indicates the exchange mechanism is not the sole basis for multimodal behavior.

The multimodal behavior observed in this work was not observed in previous work on telechelic and statistical PDMS networks with mixed crosslinkers.[16] A schematic of a telechelic network similar to our prior work shows each strand only connected to the network at two dynamic bond sites (**Figure 5c**). The strand exchanging via a fast crosslinker will disengage the polymer from the network before the effects of the slower bond exchange occur. Our PDMS telechelic network with mixed crosslinkers (four orders of magnitude difference in exchange kinetics) only showed one relaxation mode closer to that of the pure fast network.[16] Pendant or statistically crosslinked vitrimers can have more than two crosslinks per chain and have more opportunities for multiple exchange processes to determine the relaxation spectra. Kalow and coworkers used a statistical PDMS network with crosslinkers of multiple orders of magnitude kinetics and did not observe multiple modes in the mixed networks when kinetics were close (**Figure 5d**).[15] In this work, there were approximately two crosslinks per chain, which could contribute to the non-hierarchical behavior. The acrylate boronic ester networks in this work have statistical crosslinking with approximately 10 bonding sites and do lead to multiple relaxation modes, which points to the importance of polymer architecture on dynamic design.

Conclusions

Hierarchical dynamics were achieved in dry vitrimers through a combination of using fast and slow crosslinkers with three orders of magnitude difference in kinetics, more than two dynamic

bonds per strand, and a statistically crosslinked chemistry rather than telechelic. To further probe the mechanisms behind multimodal relaxation behavior, future work could mix types of exchange such as associative and dissociative mechanisms and mix more than two types of crosslinker in one network. Careful attention to the polymer architecture and chemistry of these networks produced successful multi-modality of relaxation, and these design parameters can be easily translated to various types of materials in the future. The ability to tune the number and breadth of peaks in the relaxation spectrum is important for future design of polymers for applications from vibration and sound damping to adhesives and soft robotics. Deeper understanding of bulk phenomena characteristics from microstructural changes will help design complex soft materials.

Methods

Synthesis of 2,3-dihydroxypropyl acrylate: To a stirring solution of DL-1,2-isopropylideneglycerol (75.6 mmol) and Et3N (13.7 ml) in 50 ml dry flask filled with dichloromethane backfilled with nitrogen gas and in an ice bath, acryloyl chloride (75.8 mmol) was added dropwise. The solution was allowed to warm up to room temperature overnight. The mixture was diluted with dichloromethane. The organic layer was washed with water, dried over sodium sulfate, and evaporated in vacuum. The product was dissolved in a mixture of 1:1 75.8 ml THF and 75.8 ml HCl (4M) and stirred at room temperature overnight. Excess sodium carbonate was added to neutralize the produced hydrochloric acid. The mixture was crashed out with THF, dried by sodium sulfate, and evaporated under vacuum. The crude product was purified by column chromatography (EA:Hexane = 1:1) to yield a pale yellow liquid.

Synthesis of butyl acrylate homopolymer: Butyl acrylate monomer (Sigma Aldrich, 128.17 g/mol) was weighed (8 grams) into a 100mL flask. A degree of polymerization of 105 (Mw = 13,500

g/mol) with 10% crosslinking diol sites was targeted. The synthesized acrylate diol was added in 1:10 ratio to the butyl acrylate monomer. The RAFT agent, 4-cyano-4-[(dodecylsulfanylthiocarbonyl)sulfanyl]pentanoic acid was added in 1/105 ratio to the monomer, and the AIBN initiator (azobisisobutyronitrile) was added in a 1/5 ratio to the RAFT agent (1:525 weight ratio to monomer). The solvent dimethylformamide was added to the mixture of these components in the vial in a 1.2 M ratio. The vial was closed with a rubber stopper and a needle to bubble nitrogen air into the solution and a venting needle were added through the top of the stopper. The vial was placed in a silicone oil bath at 250rpm with no temperature. Nitrogen air was bubbled through the system for 30 minutes to remove any oxygen from inhibiting the reaction. The nitrogen needle was removed, and the venting needle was attached to the closed Schlenk line to create a closed system with a slight positive pressure. The vial mixed at 80°C for 3-4 days. Then, the vial was placed in the fridge overnight. The solution was crashed out in 150mL H_2O and then collected and dried overnight in a vacuum oven at 100°C until the solution was clear and yellow.

Synthesis of fast crosslinker*:* The boronic ester with nitrogen moieties was adapted from Guan and coworkers[18] and follows the synthesis mentioned in a previous paper.[16]

Synthesis of crosslinked acrylate network*:* The acrylate homopolymer was placed in a 20mL vial heated at 60°C on a hot plate. Crosslinker percentage was calculated as the number of -OH groups per polymer chain divided by the functionality of the crosslinker. The ratio here was 4.36:1 crosslinker to polymer. The crosslinker was weighed out into a separate 20mL vial and filled with 10mL of ethanol. The crosslinker/ethanol vial was placed in the sonicator at 40℃ for approximately 1 hour or until the crosslinker had dissolved. A plastic pipette was used to add the crosslinker/ethanol mixture to the acrylate vial on the hot plate. A stir bar was added and stirring was set to 350rpm. The mixture was allowed to mix at 60°C while capped for five hours. The vial

was uncapped, and the temperature was increased to 90°C overnight. When the ethanol had dissolved, the vial was moved to a vacuum oven set to 120°C for 12 – 18 hours.

Rheology of acrylate networks*:* The rheology for these samples was performed on a TA DHR-2 instrument in the linear regime found from oscillatory amplitude sweeps. To prepare each sample for rheology, 0.2 – 0.5 grams of material was placed into an 8mm diameter disk mold and pressed using a hydraulic hot press set to 80°C for 5 – 10 minutes to ensure a uniform sample. The sample was quickly cut out of the mold and placed onto the calibrated bottom plate of the 8mm parallel plates geometry. The rheology tests were run from high to low temperatures. A frequency sweep was performed at each decade of temperature between 80 and 0°C and between 100 and $1 \cdot 10^{-3}$ or $5 \cdot 10^{-4}$ Hz.

REFERENCES

1. Ewoldt, R. H.; Saengow, C., Designing Complex Fluids. *Annual Review of Fluid Mechanics* **2021,** *54* (1).
2. Ligon, S. C.; Liska, R.; Stampfl, J.; Gurr, M.; Mülhaupt, R., Polymers for 3D Printing and Customized Additive Manufacturing. *Chemical Reviews* **2017,** *117* (15), 10212-10290.
3. Tan, L. J.; Zhu, W.; Zhou, K., Recent Progress on Polymer Materials for Additive Manufacturing. *Advanced Functional Materials* **2020,** *30* (43).
4. Blaiszik, B. J.; Kramer, S. L. B.; Olugebefola, S. C.; Moore, J. S.; Sottos, N. R.; White, S. R., Self-Healing Polymers and Composites. *Annual Review of Materials Research* **2010,** *40* (1), 179-211.
5. Wang, S.; Urban, M. W., Self-healing polymers. *Nature Reviews Materials* **2020,** *5* (8), 562-583.
6. Kim, J.; Kim, J. W.; Kim, H. C.; Zhai, L.; Ko, H.-U.; Muthoka, R. M., Review of Soft Actuator Materials. *International Journal of Precision Engineering and Manufacturing* **2019,** *20* (12), 2221-2241.
7. Monkman, G. J., Advances in shape memory polymer actuation. *Mechatronics* **2000,** *10* (4-5), 489-498.
8. Bruce, P. G.; Vincent, C. A., Polymer electrolytes. *Journal of the Chemical Society, Faraday Transactions* **1993,** *89* (17).
9. Hallinan, D. T.; Balsara, N. P., Polymer Electrolytes. *Annual Review of Materials Research* **2013,** *43* (1), 503-525.
10. Wake, W. C., Theories of adhesion and uses of adhesives: a review. *Polymer* **1978,** *19* (3), 291-308.

11. Chung, D. D. L., *Journal of Materials Science* **2001,** *36* (24), 5733-5737.
12. Sperling, L. H., Sound and Vibration Damping with Polymers. In *Sound and Vibration Damping with Polymers*, 1990; pp 5-22.
13. Grindy, S. C.; Learsch, R.; Mozhdehi, D.; Cheng, J.; Barrett, D. G.; Guan, Z.; Messersmith, P. B.; Holten-Andersen, N., Control of hierarchical polymer mechanics with bioinspired metal-coordination dynamics. *Nature Materials* **2015,** *14* (12), 1210-1216.
14. Yesilyurt, V.; Ayoob, A. M.; Appel, E. A.; Borenstein, J. T.; Langer, R.; Anderson, D. G., Mixed Reversible Covalent Crosslink Kinetics Enable Precise, Hierarchical Mechanical Tuning of Hydrogel Networks. *Advanced Materials* **2017,** *29* (19).
15. El-Zaatari, B. M.; Ishibashi, J. S. A.; Kalow, J. A., Cross-linker control of vitrimer flow. *Polymer Chemistry* **2020,** *11* (33), 5339-5345.
16. Porath, L.; Huang, J.; Ramlawi, N.; Derkaloustian, M.; Ewoldt, R. H.; Evans, C. M., Relaxation of Vitrimers with Kinetically Distinct Mixed Dynamic Bonds. *Macromolecules* **2022,** *55* (11), 4450-4458.
17. Davies, A. R.; Anderssen, R. S., Sampling localization in determining the relaxation spectrum. *Journal of Non-Newtonian Fluid Mechanics* **1997,** *73* (1-2), 163-179.
18. Cromwell, O. R.; Chung, J.; Guan, Z., Malleable and Self-Healing Covalent Polymer Networks through Tunable Dynamic Boronic Ester Bonds. *Journal of the American Chemical Society* **2015,** *137* (20), 6492-6495.
19. Winter, H. H., The Critical Gel. In *Structure and Dynamics of Polymer and Colloidal Systems*, 2002; pp 439-470.
20. Freund, J. B.; Ewoldt, R. H., Quantitative rheological model selection: Good fits versus credible models using Bayesian inference. *Journal of Rheology* **2015,** *59* (3), 667-701.
21. Martinetti, L.; Soulages, J. M.; Ewoldt, R. H., Continuous relaxation spectra for constitutive models in medium-amplitude oscillatory shear. *Journal of Rheology* **2018,** *62* (5), 1271-1298.
22. Wang, Y.; Kaur, A. P.; Attanayake, N. H.; Yu, Z.; Suduwella, T. M.; Cheng, L.; Odom, S. A.; Ewoldt, R. H., Viscous flow properties and hydrodynamic diameter of phenothiazine-based redox-active molecules in different supporting salt environments. *Physics of Fluids* **2020,** *32* (8).
23. Ramlawi, N.; Bharadwaj, N. A.; Ewoldt, R. H., The weakly nonlinear response and nonaffine interpretation of the Johnson–Segalman/Gordon–Schowalter model. *Journal of Rheology* **2020,** *64* (6), 1409-1424.
24. Singh, P. K.; Soulages, J. M.; Ewoldt, R. H., On fitting data for parameter estimates: residual weighting and data representation. *Rheologica Acta* **2019,** *58* (6-7), 341-359.
25. Montarnal, D.; Capelot, M.; Tournilhac, F.; Leibler, L., Silica-Like Malleable Materials from Permanent Organic Networks. *Science* **2011,** *334* (6058), 965-968.
26. Li, L.; Chen, X.; Jin, K.; Torkelson, J. M., Vitrimers Designed Both To Strongly Suppress Creep and To Recover Original Cross-Link Density after Reprocessing: Quantitative Theory and Experiments. *Macromolecules* **2018,** *51* (15), 5537-5546.
27. Smith, M. K.; Northrop, B. H., Vibrational Properties of Boroxine Anhydride and Boronate Ester Materials: Model Systems for the Diagnostic Characterization of Covalent Organic Frameworks. *Chemistry of Materials* **2014,** *26* (12), 3781-3795.